A PROPOSAL TO SEARCH FOR THE NEUTRAL HEAVY BOSON Z^o

U.J. Becker, P.J. Biggs, G. Everhardt, P. Goldhagen. R. Little and S.C.C. Ting.

Laboratory for Nuclear Science, Massachusetts Institute of Technology, Cambridge, Massachusetts 02139,USA

Abstract: We propose to set-up a large solid angle parasite detector outside the split-field-magnet to search for massive $40 \geq M_{Z^o} \geq 10$ BeV neutral vector mesons by detecting its large opening angle ($180^o \geq \theta \geq 100^o$) decay mode $Z^o \rightarrow \mu^+\mu^-$ with energy of μ larger than 5 BeV/c.

It is intended to run this detector outside the SFM and does not interfere with its operations.

Theory: The existence and the mass of Z^o.

Recent development in unified gauge theories [1-7] of weak and electromagnetic interactions have been fruitful in focusing attention on the experimental question of the existence of leptonic and hadronic neutral currents.

The Weinberg-Salam model [1,2] requires a neutral Z^o coupled to $\bar{\nu}\gamma_\mu(1-\gamma_5)\nu$, without any additional leptons besides e, ν_e, μ, ν_μ. The mass of Z^o is $M_{Z^o} = 37$ GeV/ $|\sin\theta|$ with $\tan\theta = \frac{g'}{g}$: where g', g

are coupling constants. The mass of Z^o is bounded below by 74 GeV.

The Georgi-Glashow [4] model requires two kinds of heavy leptons; the electron-type E^o, E^+ with $n_e = +1$; and the muon-type M^o, M^+ with $n_\mu = +1$. It has no additional neutral bosons. The g-2 experiment implies $\frac{M_{M^+}}{M_W} \leq \frac{1}{10}$, $\frac{M_{E^+}}{M_W} \leq 1/2$.

The Bjorken-Llewellyn-Smith and the Lee-Prentki-Zumino models [5,6,7] require both Z^o and heavy leptons. There is no theoretical lower bound on the mass of Z^o. Primack and Quinn [10] have analysed the g-2 experiment for electrons and muons and have found that the present experimental accuracy gets a mass limit of $M_{Z^o} \geq 10$ GeV.

In all these models there is a neutral scalar boson φ^o, (the Higg's particle). The mass of φ^o is a free parameter of the model.

B. The Properties of Z^o.

Z^o should be coupled directly to $\mu^+ \mu^-$ (this is quite different from the usual vector meson decays via one photon $\rho \rightarrow \gamma \rightarrow e^+e^-$). Thus the reaction $p + p \rightarrow \mu^+\mu^- X$ and $P + P \rightarrow Z^o + X$ should be similar to each other.

The integrated production cross section for μ pairs with mass greater than Q_o^2 is enhanced by a factor of approximately $\alpha^{-1} (\frac{M^2}{Q_o^2})$ for production via Z^o relative to production via a virtual photon.
The factor α is the usual (mass/width) enhancement from production of the resonance. The factor M^2 / Q_o^2 appears because the virtual photon channel falls relative to the Z^o channel at increasing Q^2 (a result of the photon propagation).

The width of Z^o is narrow, typically $\Gamma = \alpha M$, where α is the fine structure constant.

In the paper of Jaffe and Primack [11] we list all the other properties of Z^o, E^o, E^+, M^o, M^+, φ^o as reference.

C. Production cross section of Z^o.

One can calculate the production of Z^o following the Parton (and Quark) model of Kuti and Weisskopf [12].
In this model protons are made of Quarks, Antiquarks, gluons, etc.
The production of Z^o comes from parton-antiparton annihilations. The distribution of partons is given by the SLAC deep inelastic scattering data.
The validity of this model has been checked against the Brookhaven $p + p \rightarrow \mu^+\mu^- + X$ data.

Jaffe and Primack have carried out the calculation for this experiment [11].
Assuming scaling in the form factors, one has

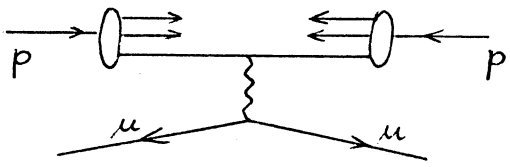

$$\frac{d\sigma}{dQ^2} = \sigma_{Q\bar{Q}\rightarrow\mu^+\mu^-}(Q^2) \int dx_1 dx_2 \sum_a \frac{F_{2a}(x_1)\, F_{2a}(x_2)}{\lambda_a^2\, x_1\, x_2} \delta\left([p_1 + p_2]^2 - Q^2\right) \qquad (1)$$

In the detailed calculation of the Z^o yields they have modified the theory to take into account:

(1) the upper limit of ISR $pp \rightarrow e^-e^+ X$ experiment [13,14] and

(2) the threshold cut off effects when $\sqrt{s} \approx M_{Z^o}$ has been carried out for our particular experimental condition of 28 GeV - 28 GeV ISR beam, $s = 3130\ (\mathrm{GeV/c})^2$.

The following table lists the typical total cross section σ for the production of Z^o as function of mass. Using P_{ISR} = 28 GeV (S = 56 GeV)[15]

M_{Z^o} = 15 GeV	$\sigma = 2 * 10^{-34}$	cm^2
M_{Z^o} = 20 GeV	$\sigma = 1 * 10^{-34}$	cm^2
M_{Z^o} = 30 GeV	$\sigma = 2 * 10^{-36}$	cm^2
M_{Z^o} = 37 GeV	$\sigma = 3 * 10^{-37}$	cm^2

Table I gives some examples of the decay kinematics of Z^o.

Experimental set up

To detect Z^o we propose to set up one (or both) of the following two possible parasite spectrometers, to run together with any of the currently approved SFM experiments.

(I) One possibility is to set up a muon detector outside the split-field-magnet detector to detect the $Z^o \longrightarrow \mu^+ \mu^-$. Fig. 1 shows the top view of the spectrometer.

H_1, H_2, H_x, H_y are plastic scintillator hodoscopes which were designed to study particle correlations in the pionization region at the ISR (see CERN/ISRC/71-37).

H_3, H_4, H_z, H_w are additional liquid scintillation counters. The time resolution of such a detector can be done to 1 ns (see Appendix 1). The sizes of them are given in Table II.

There are 60 hodoscopes in each H_3 and H_z to improve π rejection. Pions interacting in the concrete before H_3 and H_z events can be rejected by requiring only one hodoscope signal from each H_3 and H_z. In front of each liquid scintillation counter there are about 3 meters of concrete. The 6 meter of concrete is used to identify muons with energies greater than 5 BeV.

The selection of events is done as follows:

1) Hodoscopes H_1, H_2, H_3, H_4 define a μ track with energy > 5 BeV.

2) The mass selection is done by coincidences H_1, H_2, H_3, H_4 with H_x, H_y, H_z, H_w located on the opposite side of the SFM: with opening angles greater than 80^o, it can be simply visualized as follows:

Triggering system of $Z_o \rightarrow \mu^+ \mu^-$ for arrangement 1 .

Define counter No. I: clockwise in the x-z plane

hodoscope	no. of counter	I	$\Delta\theta$ each counter	$\Delta\varphi$
H_3	60	1-60	$\pm 1.3^o$	$\pm 22^o$
H_z	52	77-128	$\pm 1.3^o$	$\pm 17^o$

$$\text{trigger} = \left[(H_1 \cdot H_2 \cdot H_3 \cdot H_4) \text{ or } (H_x \cdot H_y \cdot H_z \cdot H_w)\right] * (32 < |\Delta I| < 108)$$
$$*((H_1+H_x) \geq 2) * ((H_2+H_y) \geq 2) * ((H_3+H_z) = 2)$$
$$*((H_4+H_w) = 2)$$

which selects muon pairs with opening angle greater than 80^o and energies of the muon greater than 5 BeV.

3) The size of the hodoscopes and wire spark chambers, excluding the central region between 80^o to 90^o where the momentum resolution is very poor, coers a region of 2 steradians. With the knowledge of the location of the particles given by track reconstruction, the timing information of 1 ns will be done by putting two tubes at each end of the triggering counters. This together with the SFM detector information on the interaction vertex will enable us to reject cosmic ray backgrounds. The final analysis will be done with SFM chamber information. The location of the interaction point is defined by the reconstruction in the SFM chambers. The momentum resolution and mass resolution are given in Tables IIIa and IIIb.

Counting Rate. The yields with luminosity of 10^{31} cm $^{-2}$ sec^{-1} and 10^5 sec/day are typically (with $\frac{\Delta\Omega}{4\pi}$ = 18%).

M_{Z^o} (GeV)		rate/day	rate/100 days
15	$2\times10^{-34}\times10^{5}\times10^{31}\times\frac{\Delta\Omega}{4\pi}$	= 36 /day	3600
20	$10^{-34}\times10^{5}\times10^{31}\times\frac{\Delta\Omega}{4\pi}$	= 18/day	1800
30	$2\times10^{-36}\times10^{5}\times10^{31}\times\frac{\Delta\Omega}{4\pi}$	= 0.3/day	30
37	$3\times10^{-37}\times10^{5}\times10^{31}\times\frac{\Delta\Omega}{4\pi}$	= 0.05/day	5

Background. One calculates the background from two sources:

Background from π, K decay in flight: using the ISR π, K inclusive data [16], one can calculate the number of muons from π, K decay. Number of muons from π, K decay.

$$= \sum_{\pi,K} \begin{pmatrix} \text{decay} \\ \text{probability} \\ \text{after 5 meters} \end{pmatrix} \left(\int \left[E_\pi \frac{d^3\sigma}{dp_\pi^3} \right] \frac{p_\pi^2}{E_\pi} dp_\pi \right) (\Delta\Omega)(L)(10^5 \text{ sec/day})$$

where $E_\pi \frac{d^3\sigma}{dp^3}$ is the invariant cross section for inclusive π cross section

L = luminosity = 10^{31} cm^{-2} sec^{-1}

The K yield at large $p_\perp$ is the same as π . The life time of K is much shorter than π meson. However, because of the large mass difference between the kaon and the muon, the momentum of muon from K^{+}_{-} decay is significantly lower than that of the original K^{+}_{-}. With a cut-off energy at 5 BeV, we found the relative muon contributions from K^{+}_{-} decay and from π^{+}_{-} decay is

3. It is close to the intersecting beams so that the kaons and pions are absorbed before they have the chance to decay. The probability for a 5 GeV kaon and pion to decay before being absorbed is $<1.2\%$ and $<.2\%$, respectively.

4. Having the muon filter close to the intersection region, enables us to cover a large solid angle with reasonable size of counters and spark chambers.

In Figures 3,4 we show the side views of such a detection system. The size of counters and chambers are listed in Table 6.

To select events , we arrange the counters in the following way:

	number of counters (two tubes on each end)	size of each counter	counter number I
A1	7	1m x 3.8m	1 - 7
A2	7	1m x 3.8m	8 -14
A3	3	1m x 3.8m	27 -29
A4	6	1m x 38 m	21 -26
A5	3	1m x 38 m	18 -20

$\Delta\theta = \pm 5^{o}$

$\Delta\varphi = \pm 25^{o}$

Trigger = $((U * (A_1 + A_2))$ or $(D * (A_3 + A_4 + A_5)))$ * $((A_1 + A_2 + A_3 + A_4 + A_5) = 2)$ $(28 > \Delta I > 9)$ where U and D are two hodoscope counters above and below the intersection region in the SFM. This trigger selects muon pairs with opening angle greater than 80^{o} and each muon energy greater than 5 BeV.

The initial directions of the $\mu^{\pm}$ are measured by the proportional chamber system inside the SFM to an accuracy of $\approx \pm 7$ mr.

The muon tracks also determine the interaction vertex to a few mm. The directions outside the magnet are measured by two sets of wire spark chambers. Between the spark chambers there may be a second hadron filter or a range absorber for low energy μ mesons of approximately 30 cm of iron. Scintillation counters are behind the spark chambers, which together with hodoscope counters around the intersection inside the SFM define a muon pair produced from beam beam interaction. The relative timing using meantimers between the top and bottom counters rejects single cosmic rays which go through the beam interaction region as well as the whole detector system.

The solid angle covered by the tentative arrangement of the counters shown in Fig. 3 and Fig. 4 is 3 ster. The details of the size and support for the detector system still has to be worked out with the SFM groups.

To first order momentum resolution is dominated by multiple scattering in the 166 X_o of iron. The effect of multiple scattering is $\theta_s = \frac{15}{p}\sqrt{166}$ mrad. For $28 > p > 5$ GeV: $7 < \theta_s < 40$ mrad, which is much larger than the angular measurement errors from chambers outside the iron. With 47 KGM of field, the μ bends an angle $\theta_p = \frac{30*47}{p}$ mrad.

the $\frac{\Delta p}{p} = \frac{\theta_s}{\theta_p} = \frac{15*\sqrt{166}}{30*47} = \pm 13\%$.

The opening angle is measured by the SFM detector to ± 10 mr. Thus the mass resolution is $\frac{\Delta m}{m} = \frac{1}{\sqrt{2}}\frac{\Delta p}{p} = \pm 10\%$. This is true for mass of Z_o $\geq$ 25 GeV, when the effect of energy loss is small.

Higher order corrections included energy loss in the iron, scattering over extend body, detailed knowledge of field mapping, are being calculated with existing standard programs.[17]

One notes that if evidence of Z^o is found, one can measure the multiple scattering, energy loss, and magnetic fields by two ways:

(1) at large angle: by installing a magnet under the SFM and study the cosmic ray flux.

(2) at small angle: by measuring the μ distribution outside SFM from the known $\pi \rightarrow \mu$ decay in the SFM.

The solid angle of the detector is 1.3 times larger than the previous one. The counting rate of this detector is $\lesssim$ 1.3 times larger than those listed on page 6 accordingly.

To calculate the background from $K \rightarrow \mu$, $\pi \rightarrow \mu$, we note that:

(1) the decay length is short;

(2) the $\frac{\Delta p}{p} \approx 13\%$.

These two effects tend to cancel each other.

In Table VIIa we list the muon yield from π and K decays. In Table VIIb we list the integrated muon pair yield calculated in the same way as before, and finally in Table VIIc we list the signal to background rate, and the total signal rate for this set-up.

The two set-up have different relative merits. In set-up I: the momentum and angle of muon is measured accurately. The $\frac{\Delta m}{m}$ resolution is < 3.5%. The decay length is longer. The $\frac{K}{\pi} \rightarrow \mu^{\pm}$ accidentals under the Δm is small. In set-up II, the momentum and angle are not so well measured. Leading to $\frac{\Delta m}{m} \approx 10\%$, but the 4 m of iron form a good shielding and the decay correction, because of short decay path, is very small. Thus the best approach is to set-up both, either simultaneously or one after the other.

Finally we remark on the problem of cosmic ray background. The only cosmic rays that will trigger our system is the hard muons with energy $>$10 BeV. We can reject this background by the following methods:

1. Requiring directional timing information of 1 ns.

2. The SFM detector gives us a precision measurement of angle. A straight through cosmic-ray muon will have an angle of exactly 180^{o}. By selecting events away from a straight line we will reject the single muons.

3. With the cosmic ray information from the single muon experiment at the ISR we have estimated that the contribution from muon background is $\ll$ than 10 % in all cases.

Time schedule: We hope to be able to start testing the setup in the middle of 1974 and will run 1974-1975 on parasite base.

Acknowledgements:

We are grateful for the calculations of Dr. R.J. Jaffe and Dr. Joel Primack who have made this proposal possible.

We acknowledge conversations with Dr. V.F. Weisskopf, Dr. R. Jackiw, Dr. S. Weinberg, Dr. T.T. Wu, and Dr. M. Deutsch.

References:

1. A. Salam, in Elementary Particle Theory, edited by N. Svartholm (Almquist and Forlag, Stockholm, 1968).
2. S. Weinberg, Phys. Rev. Letters 19, 1264 (1967); 27, 1688 (1971); Phys. Rev. D 5, 1412 (1972); 5, 1962 (1972).
3. G. 't Hooft, Nucl. Phys. B35, 167 (1971).
4. H. Georgi and S.L. Glashow, Phys. Rev. Letters 28, 1494 (1972).
5. B.W. Lee, Phys. Rev. D 6, 1188 (1972).
6. J. Prentki and B. Zumino, Nucl. Phys. B47, 99 (1972).
7. For references to some of the other papers on this subject which had appeared in early 1972, see: B.W. Lee, NAL Report No. THY-34, 1972 (invited paper presented at the San Francisco meeting of the APS, 1972); C.H. Llewellyn Smith, in Proceedings of the Fourth International Conference on High Energy Collisions, Oxford, 1972 (Oxford Univ. Press, to be published).
8. T.D. Lee, P.R.L. 26, 801 (1971).
9. Schwinger: P.R. Vol. 7, No. 3, p. 908, 1972.
10. J. Primack and H. Quinn, Phys. Rev. Letters D6, 3171 (1972).
11. J. Primack and R.L. Jaffe, to be published in Nuclear Physics, 1973.
12. J. Kuti and V.F. Weisskopf, Phys. Rev. D4, 3418 (1971).
13. R.L. Jaffe, MIT preprint CTP 344 (1973).
14. see foot note 11 of above reference.
15. To be conservative, we only use 1/2 of the calculated cross sections of ref. 11.
16. Endre Lillethun, Scientific/Technical Report No 47,
17. H. Øverås, CERN Report 60-18, Synchro-Cyclotron Division 10 May, 1960

TABLE I

Decay Kinematics for Z^o

From $M^2 = 2P_+P_-(1-\cos\theta_{+-})$ where θ_{+-} is the opening angle between P_+ (momentum of μ^+) and P_- (momentum of μ^-) we obtain:

M(BeV)	θ_{+-}	Range of momentum * accepted by the detector $P_{\pm}$ (BeV/c)	Range of Z^o momenta accepted by the detector (BeV/c)
15	180^o	5.0 to 11.3	0 to 6.3
	160^o	5.0 to 11.6	2.6 to 7.1
	140^o	5.0 to 12.7	5.5 to 9.4
	120^o	5.0 to 15.0	8.7 to 13.2
	100^o	5.0 to 19.1	12.6 to 18.9
	80^o	all +	17.9 to 26.
20	180^o	5.0 to 20	0 to 15
	160^o	5.0 to 20.6	3.5 to 16
	140^o	5.0 to 22.6	7.3 to 19.1
	120^o	all	11.5 to 24.
30	180^o	8.0 to 28.0	0 to 20
	150^o	all	8.0 to 20
40	180^o	14.3 to 28.0	0 to 13.7
	150^o	all	10.7 to 13.7

* The maximum momentum is limited by kinematics. The minimum momentum is limit ed either by the degrader or kinematics.

\+ "All" means all kinematically possible values are accepted.

TABLE II

Counter Sizes and Angular Acceptance

Counter (liquid scintillator)	No. of hodoscopes	sizes of hodoscopes		
		width	height	thickness
H_3	60	.37 m	6.6 m	15 cm
H_4	12	2.66 m	9.4 m	15 cm
H_z	52	.38 m	5.1 m	15 cm
H_w	12	2.33 m	7.3 m	15 cm

$\Delta\Omega$ of H_3, H_4 = 1.3 sr
$\Delta\Omega$ of H_z, H_w = 0.98 sr
} 18% of 4π

TABLE IIIa

High momentum resolution of tracks leaving in angular range 30° - 70° in C.M. system

	Δ p/p in %				
	Θ cm				
P_{CM}	30°	40°	50°	70°	
1 GeV/c	.3	.4	4.3	10	
3 GeV/c	.8	.9	1.4	6.3	Q = -1
6 GeV/c	2.9	1.6	2.5	9.4	$\phi = -80^{\circ}$
10 GeV/c	4.4	2.5	3.9	15.2	
1 GeV/c	.3	.4	2.6	5.3	
3 GeV/c	.7	.9	1.3	7.5	Q = -1
6 GeV/c	3.1	1.4	2.4	5.4	$\phi = -90^{\circ}$
10 GeV/c	4.7	2.6	4.0	10.2	

We have used SFM detector + 1 outer chamber at x = -446 cm from the intersection region with forward chambers 2 mm wire spacing and central and outer chambers 4 mm wire spacing.

P_{CM} is total CM momentum, Θ and ϕ are defined in the SFM coordinate system (see Fig. 2).

TABLE IIIb

Mass resolution for symmetric pairs at θ cm = 40^{o} for each muon

Mass (BeV)	$\pm \frac{\Delta M}{M}$ in %
10	1.1%
20	1.8%
30	2.7%
40	3.5%

TABLE IV

(a)

Muon Rates from π,K Decay (rate per BeV per sr per day)

μ momentum / angle	7.5 BeV	10 BeV	15 BeV	20 BeV
90^o	5	0.03	-	-
60^o	15	0.8	9×10^{-3}	-
45^o	150	4.8	0.04	-
30^o	4000	140	1.22	10^{-2}

(b)

Upper limit of muon pair rates from π, K decay (rate per BeV per sr per day) = integrated single μ rates times the decay probability of a correlated π or K.

Mass (BeV)	Muon pair rates from π, K decays
15	< 20
20	< 1
30	$< 8\times10^{-3}$
37	$< 8\times10^{-4}$

TABLE V

(background taking $\Delta p = 1$ BeV)

Mass (BeV)	signal/background	
15	> 1.8	* see remarks below
20	> 18	
30	> 38	
37	> 60	

* Remarks: If we limit ourselves to those events with $\mu^{\pm}$ produced at an angle greater than 38 with respect to the proton beams, we find the event rate for M = 15 BeV is about 30 /day and the signal/background ratio becomes better than 30 as the result of the rapid decrease of $\pi^{\pm}$ yields as the transverse momentum increases.

TABLE VI

Dimensions for wire spark chambers and scintillation counters

Wire Spark Chamber	Size	Counters	Area
C1	6 m x 3.2 m	A1	7 m x 3.8 m
C2	7 m x 3.8 m	A2	7 m x 3.8 m
C3	6 m x 3.2 m	A3	3.0 m x 3.8 m
C4	7 m x 3.8 m	A4	6.0 m x 3.8 m
C5	3.2 m x 3.2 m	A5	3.0 m x 3.8 m
C6	3.2 m x 3.8 m		
C7	6.2 m x 3.2 m		
C8	6.2 m x 3.8 m		
C9	3.2 m x 3.2 m		
C10	3.2 m x 3.8 m		

TABLE VII

A. Single muon rate per day per sr per GeV

θ \ E_μ	7.5	10	15	20	(GeV)
90^o	1	6×10^{-3}	-	-	
60^o	3	0.16	1.6×10^{-3}	-	
45^o	30	1	8×10^{-3}	-	
30^o	800	27	0.24	2×10^{-3}	
19^o	cut-off	cut-off	10	0.2	
Integrate over $\Delta\Omega$	200	6.5	1.12	0.015	

B. Muon Pairs from π, K decay (upper limit per GeV^2)

Multiplied by the decay probability of the 2nd K or π	1	3.5×10^{-2}	7×10^{-3}	10^{-4}

C. Muon pair rate from π, K decay (upper limit)

$M_{\mu\mu}$ integrated over	15	20	30	40	(GeV)
$\Delta E_\mu = \pm 13\% E_\mu$ for each particle	4/day	0.23/day	0.1 /day	3×10^{-3}/day	
Event rate	43	22	0.5	0.07 2	
Signal / background	10	100	5.	24	

APPENDIX I - Time resolution in liquid scintillators

(from the work of R. Lanza and W. Kern, to be published)

In this Appendix we provide some of the technical justification for the performance of time of flight detection system by employing large counters.

Liquid scintillators are now available with light outputs and decay times comparable with those of plastic making their use practical for this application. A 3m x 3m x .5 m counter of this type has been constructed for use at NAL and this basic design can be copied. The amount of light available indicates that a timing resolution σ of $\approx .35$ ns can be obtained using reasonable care, e.g. high quality PMT's, low slewing electronics and using spark chamber data to correct for variations in timing due to geometry.

In order to evaluate the time spread which can be obtained, we calculate, using a simple model, the spread in time for a single photoelectron including time spread due to the variations in path length, decay time of the scintillator, and single photoelectron time spreads due to the phototube.

Neglecting losses at points of internal reflection one can show that the average time of arrival, $\bar{t}$, of light originating a distance L from the end is given by:

$$\bar{t} = \frac{nL}{c} \cdot \frac{n}{n-n'} \ln (n/n')$$

n = index of refraction of scintillator

n'= index of refraction of material outside sintillator

L = length

c = speed of light

with a variance $\sigma^2_{\text{Geom.}} = (\overline{t^2} - \bar{t}^2)$

$$\sigma_{\text{Geom.}} = \frac{nL}{c}\left\{\frac{n}{n'} - \left(\frac{n}{n-n'} \ln n/n'\right)^2\right\}^{1/2}$$

[The maximum time spread, $T_{Max} = \frac{nL}{c}\left(\frac{n-n'}{n'}\right)$]

for $n = 1.5$, $n' = 1$:

$\bar{t}_{\text{Geom.}} = 6L$ ns (L in meters)

$\sigma_{\text{Geom.}} = .7L$ ns

$T_{Max} = 2.5L$ ns

$n = 1.5$, $n' = 1.33$:

$\bar{t} = 5.3L$ ns

$\sigma_{\text{Geom.}} = .2L$ ns

$\Delta T_{Max} = .6L$ ns

For a scintillator with an exponential fall off of light as $e^{-t/\tau}$ one can show that:

$$\bar{t} = \tau$$

$$\sigma_{\text{Scint}} = \tau$$

For a finite thickness scintillator this becomes effectively:

$$\bar{t} = \tau + \frac{T}{2}$$

$$\sigma^2_{\text{Scint}} = \tau^2 + \frac{T^2}{12}$$

where T is the traversal time through the scintillator.

We now combine these results with experimental numbers on transit time spreads in phototubes (including variations over the photocathode) and obtain as a time spread for a single photoelectron,

$$\sigma_{SPE}^2 = \sigma_{Geom}^2 + \sigma_{Scint}^2 + \sigma_{PMT}^2$$

and consequently for N photoelectrons

$$\sigma^2 = \frac{\sigma_{SPE}^2}{N}$$

As a specific case we consider a 6m x 1m x 15cm (Fig. 5) with a scintillator $\tau \approx 2.0$ ns and estimate $\sigma_{PMT}^2 \approx 2$ for a 5" PMT, e.g. RCA 4522. More expensive tubes, e.g. C70133B have a σ^2 of ≈ 1 ns.

$$\sigma_{SPE}^2 = (1.2)^2 + (2.0)^2 + (1.4)^2 \qquad \tau = 2.0 \text{ ns}$$
$$= 7.4$$

or finally

$$\sigma = \frac{2.7}{(N)^{1/2}} \text{ns}$$

The surprising thing is that geometric effects are much less than might be supposed and in fact seem to be comparable or less than the effect of scintillator life time. (In the case of the liquid scintillator we get an advantage due to the relatively small cone into which the light is effectively emitted).

The major problem in large scintillators is then one of collecting adequate numbers of photons. Assuming a scintillator of length L and cross-section A_{Scint} <u>with no loss due to internal reflections</u>, then the number of photoelectrons at one end is:

$$N_{PE} = N_o \quad \eta \quad e^{-L/Lo} \quad \frac{\Omega}{4\pi} \quad \frac{A_{PMT}\ \text{eff}}{A_{Scint}}$$

number of photons produced	efficiency of PMT cathode	effective bulk attenuation factor	fraction of light internally reflected

(The last two factors should probably be combined into something like $\frac{\Omega_{PMT}}{4\pi}$ however the two have been separated to see the effect which devices such as light gathering cones, etc. have on performance since they may make $A_{PMT_{eff}}$ a factor of two or more over the actual area of the PMT cathode).

N_o = 6.3×10^3/cm for liquid

$\frac{\Omega}{4\pi} = \frac{n-n'}{2n}$ = .06 for liquid/Teflon

η = .2 for bialkali PMT's

$L_o \approx$ 5m for liquid

e^{-L/L_o} = 0.30 for L = 6m

Losses due to imperfect internal reflection and in light pipes and guides we estimate to be no more than a factor of two.

Liquid Scintillator

L = 6 m

A_{Scint} = .15 (1m x .15m)

assume one 5" PMT's at each end

A_{PMT} = 2 x 103 cm^2

= 206 cm^2

A_{PMT}/A_{Scint} = 0.14 (using light gathering cones should increase this by factor of 2)

$N = 15 \times 6.3 \times 10^3 \times .2 \times 0.30 \times .06 \times 1.4 \times 10^{-1}$

= 48 <u>without</u> light cones

$\approx$ 96 with light gathering cones

$\approx$ 48 with light gathering cones and including reflection losses

$\sigma_{liquid} = \frac{2.7}{(96)^{1/2}}$ = 0.28 ns

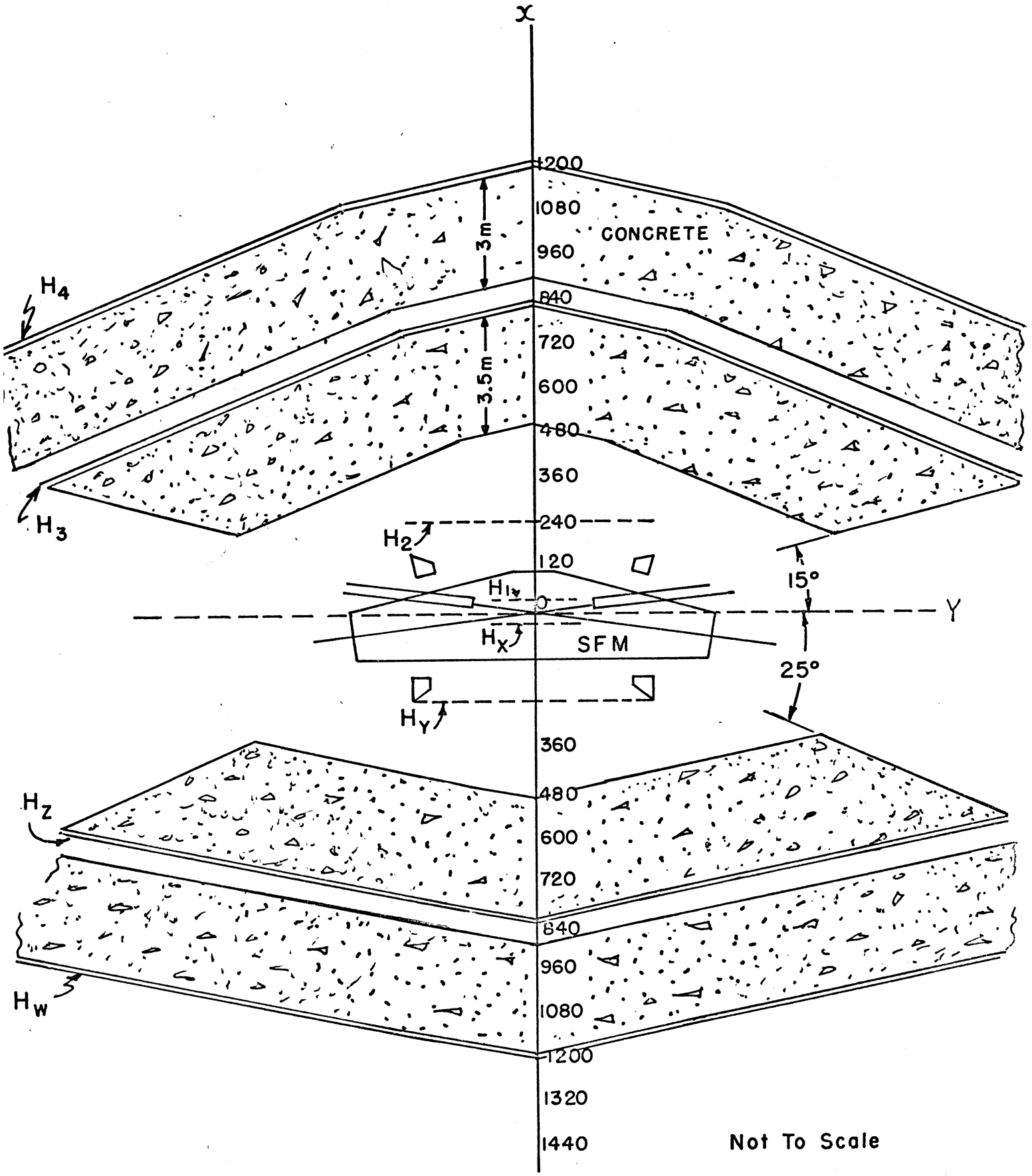
X
1200
1080
960
840
720
600
480
360
240
120
3m
3.5m
CONCRETE
H4
H3
H2
H1
HX
HY
HZ
HW
SFM
15°
25°
Y
360
480
600
720
840
960
1080
1200
1320
1440
Not To Scale

Fig 1

Coordinate System for SFM Detector

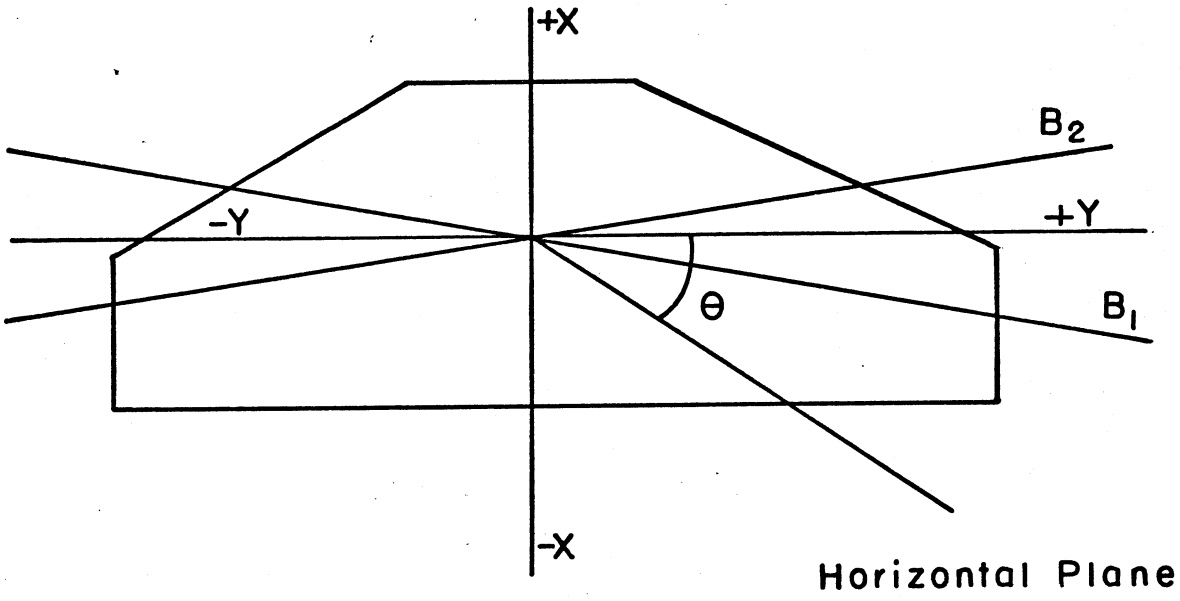

Horizontal Plane

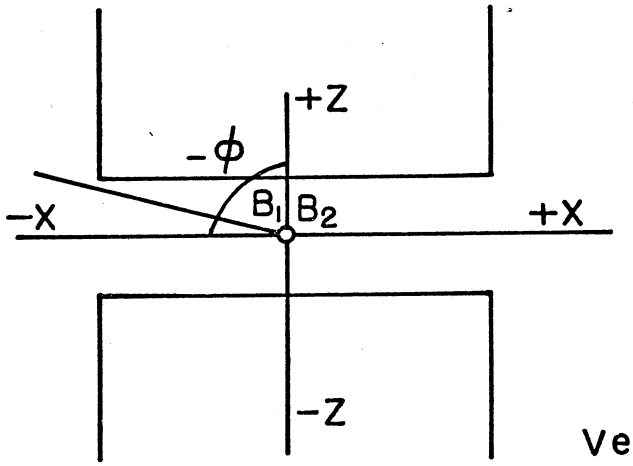

Vertical Plane

Fig. 2

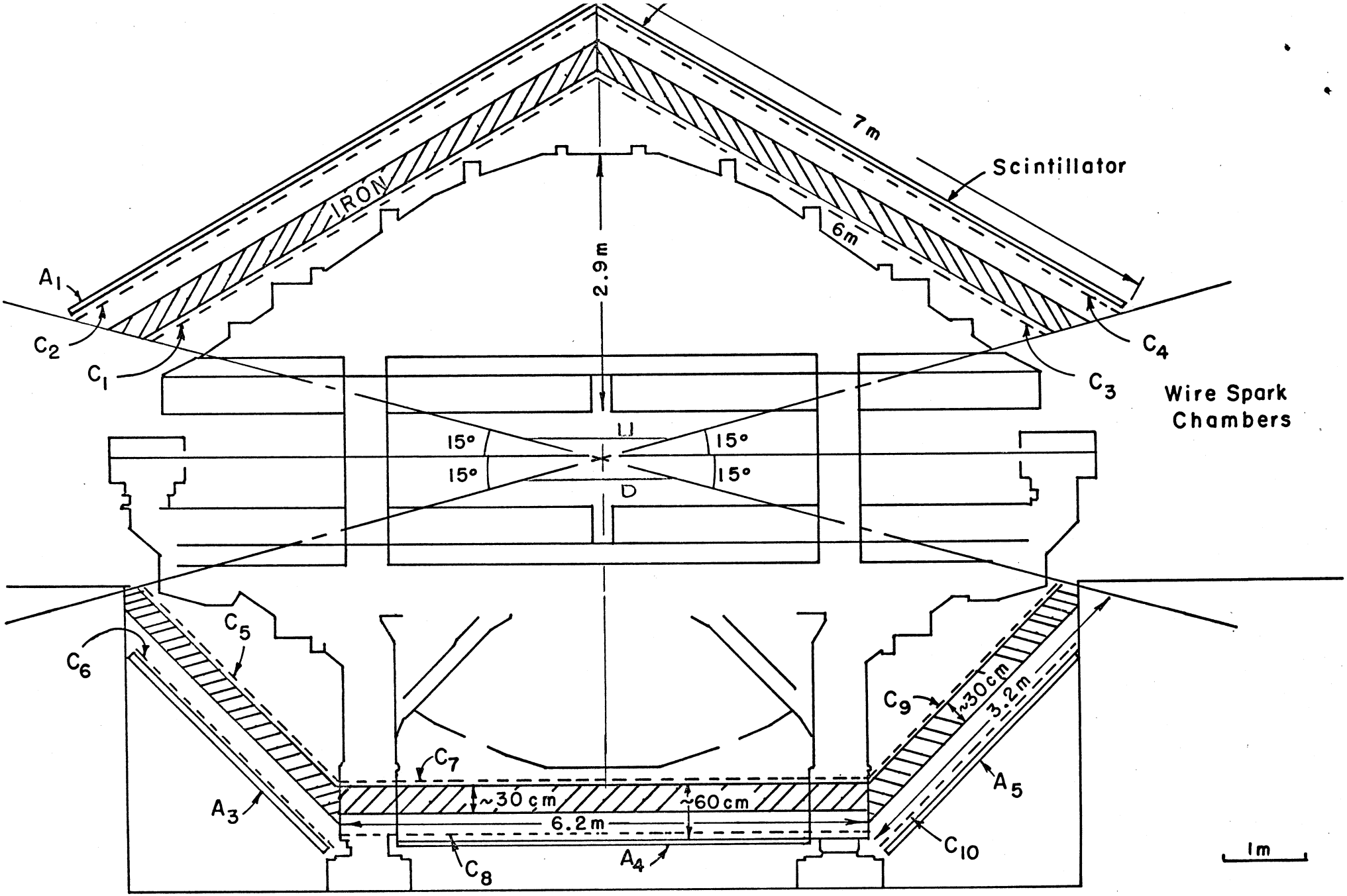
7m
Scintillator
IRON
6m
2.9 m
A1
C2
C1
C4
C3
Wire Spark
Chambers
15°
15°
15°
15°
U
D
C5
C6
C9
~30cm
3.2m
C7
A5
A3
~30 cm
~60cm
6.2m
C10
C8
A4
1m

Fig. 3

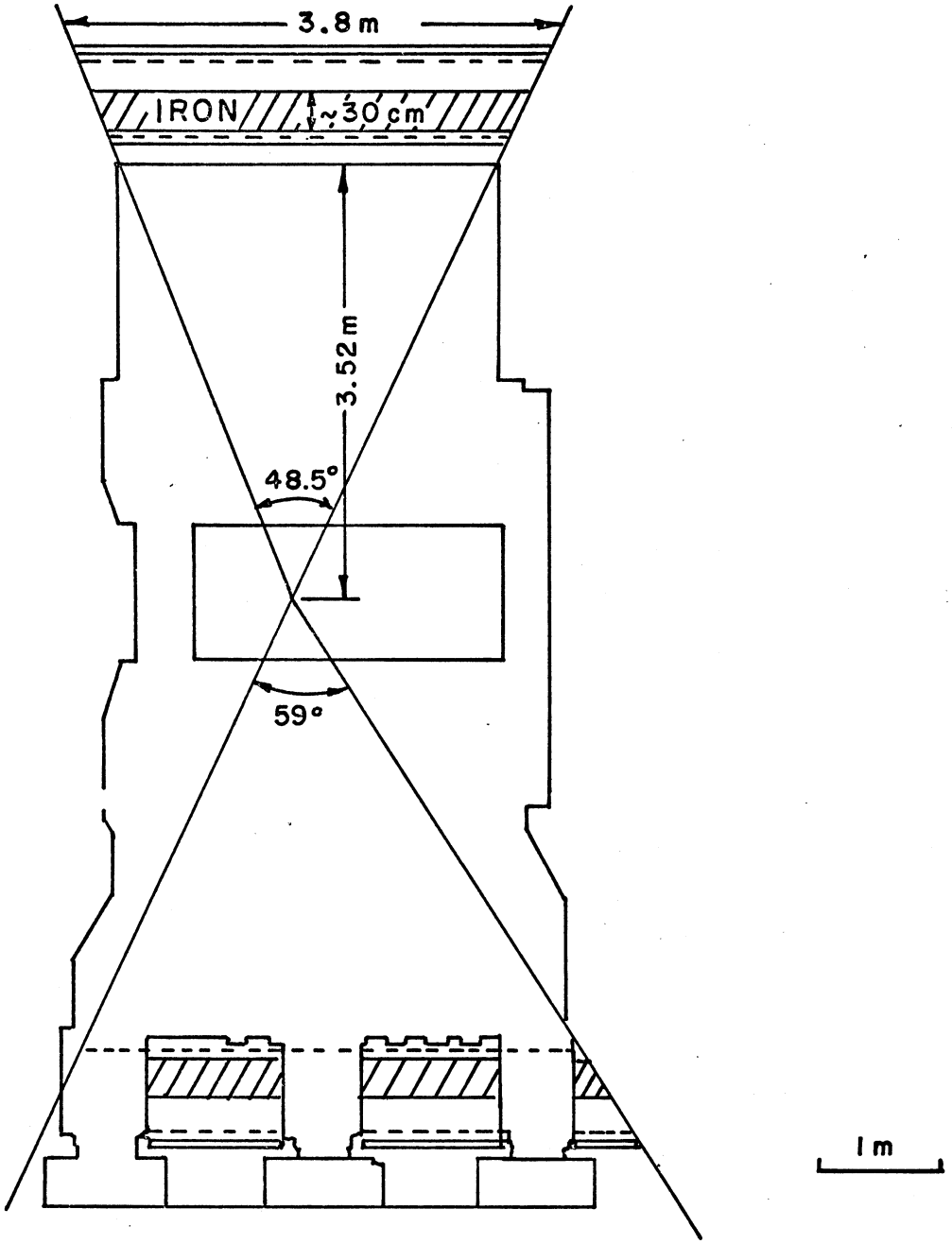

Fig. 4

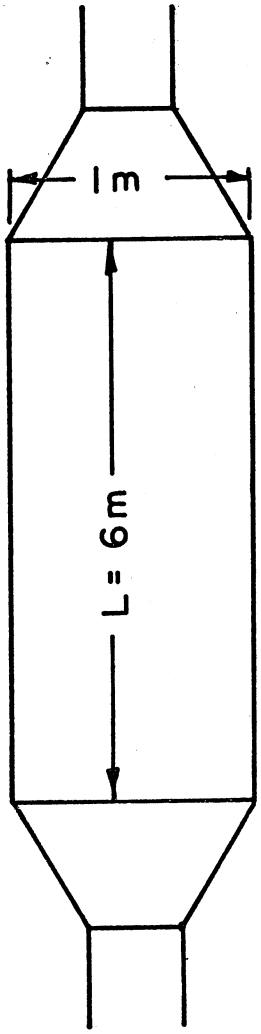

Thickness 15 cm

Fig. 5